Investigation of the mechanism of excitation of stochastic oscillations in a beam-plasma discharge

V. A. Lavrovskiĭ, I. F. Kharchenko, and E. G. Shustin

Institute of Radio Engineering and Electronics, USSR Academy of Sciences
(Submitted June 5, 1973)
Zh. Eksp. Teor. Fiz. **65**, 2236–2249 (December 1973)

We have investigated the structure of the high-frequency oscillations and of the beam-electron velocity distribution function in a beam-plasma discharge in a magnetic field. The causes of the discrepancy between the previously observed experimental results and the deductions of the nonlinear beam-plasma interaction theory are explained. It is shown that the instability characteristics measured over short time intervals agree with the predictions of the theory. The structure of the high-frequency oscillations excited in the discharge indicates that the beam interacts with a finite number of discrete plasma-oscillation modes that alternate randomly in time. The instantaneous form of the electron distribution function is a complicated multiple-hump curve. It is established that the randomization of the oscillations is due to the development of instability on the trapped particles during the nonlinear stage of the two-stream instability.

INTRODUCTION

In spite of the many theoretical and experimental studies of different aspects of plasma-beam interaction that have been performed to date, the essential details of this interaction are still not clear enough. In particular, there are appreciable discrepancies between the theoretical concepts and the experimental results, which reduce mainly to two factors. First, numerous experiments have shown that the development of beam instability in a plasma is typified by excitation of noiselike oscillations with a broad continuous frequency spectrum. This clearly contradicts the conclusions of the linear theory of coherent interaction[1], which predicts "monochromatization" of the wave packet as the wave grows[2]. Second, the smooth transformation of the distribution function of the beam electrons that is observed in these experiments – from δ-like to plateau as the instability develops – contradicts the conclusions of the nonlinear theory developed in recent years[3–6] and the results of computer experiments[7], from which it follows that the beam-electron velocity distribution function should have a complicated multiple-hump shape that varies in the course of beam relaxation.

To interpret the indicated experimental facts one resorts, as a rule, to the conclusions of the quasilinear theory of beam-plasma interaction[8–10]. Application of these conclusions to analysis of typical experiments on the interaction of a beam with a plasma is incorrect because the quasilinear theory describes only weak instability of an electron beam having a large velocity spread in a plasma, whereas in experiment one usually investigates the interaction of an almost monochromatic beam with the plasma.

In this paper we analyze the causes of the indicated discrepancies and show that the choice of the corresponding procedures for the measurements and reduction of the experimental results makes it possible to compare the characteristics of the oscillations and of the structure of the beam in a plasma-beam discharge with the conclusions of the nonlinear theory.

1. EXPERIMENTAL CONDITIONS

The experiment was performed under conditions typical of most experiments on plasma-beam discharge. The experimental setup is shown in Fig. 1. The electron beam, with energy 1 keV and current 20–40 mA, was shaped by a multielectrode gun and continuously injected into the interaction region, which was bounded by a glass tube of 2 cm diameter and 40 cm length. An electron collector, structurally combined with an electrostatic electron energy distribution analyzer, was placed at the end of the interaction region. The interaction chamber was in a longitudinal magnetic field of intensity up to 2 kOe.

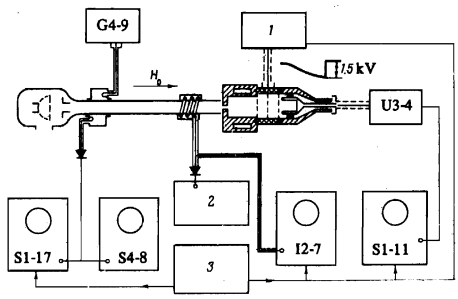

FIG. 1. Experimental setup: 1–block generating the decelerating pulse; 2–wave meter for the measurement of the averaged spectrum of the hf oscillations; 3–block of synchronizing pulses; G4-9–generator; S1-17–oscilloscope to register the plasma-density oscillations, S4-8–oscilloscope to register the plasma-density oscillation spectrum; I2-7–oscilloscope to register the oscillations of the hf field intensity; S1-11–oscilloscope to register the delay current; U3-4–amplifier.

To measure the average value of the plasma density and to study its oscillations, we used a cylindrical resonator excited at the TM_{010} mode. The mean value of the plasma density was determined from the shift of the resonant frequency. The plasma-density oscillations were registered using an inverted frequency-discrimination circuit. The exciting generator was detuned from the resonance with the plasma by an amount equal to half the resonance width. The retuning of the natural frequency of the resonator due to the oscillations of the plasma density leads in this case to oscillations of the amplitude of the resonator output-signal envelope at a constant input signal amplitude. The maximum amplitude and the upper frequency of the plasma density oscillations, registered in accordance with such a scheme, are determined by the width of the resonator-plasma resonance curve, which was of the order of 20 MHz, so that in principle it was possible to detect density changes Δn down to 5×10^{10} cm^{-3}, occurring at frequencies up to 20 MHz. The sensi-

tivity of the density-oscillation measurements was determined by the slope of the resonance curve at the operating point and amounted in our case to 10^9 cm^{-3}.

The high-frequency (hf) oscillations excited in the system upon development of the plasma-beam discharge were registered by a helical antenna wound around the glass tube. Registration of the hf oscillations with the aid of a high-speed I2-7 oscilloscope, with the oscillograms photographed in a one-shot triggering regime, made it possible to obtain realizations of the true high-frequency process of 30–100 nsec duration without any apparatus-induced transformations.

In the helium pressure range $(3-7)\times10^{-4}$ mm Hg (or $(1-3)\times10^{-3}$ mm Hg for hydrogen), injection of an electron beam with the indicated parameters produces a plasma-beam discharge. The characteristics of such a discharge were described earlier[10,11]. Notice should be taken here only of the experimental results that are important for the subsequent analysis.

Hf oscillations with different amplitudes and different statistical characteristics are registered at different instants of time at a fixed distance from the plane in which the beam is injected into the plasma. The autocorrelation functions and the spectra calculated from the oscillograms of the instability hf oscillations with periods on the order of the characteristic beam relaxation time do not agree with the spectra measured by standard inertial methods.

Simultaneously with the onset of intense hf oscillations, low-frequency (lf) oscillations of the plasma density are registered in the discharge (Fig. 2a), as well as lf oscillations of the beam current. The plasma-density oscillation amplitude depends on the discharge regime and increases in the direction of beam motion. The limits of the variation of the absolute value of the density in different discharge regimes are shown in Fig. 2b. The maximum value of $\Delta n/n$ reaches 50%.

The spectrum of the lf current oscillations occupies the range up to 4 MHz, whereas the spectrum of the plasma-density oscillations is cut off at frequencies of 150–300 kHz. The upper limit of the spectrum is due to the fact that the density oscillations have a wave character. A noticeable resonator-frequency change is observed only at frequencies at which the resonator length spans no more than one charge-density half-wave. Judging from their frequency spectrum and propagation velocity, the observed plasma-density oscillations can be identified as ion-sound waves.

2. ANALYSIS OF THE STRUCTURE OF THE hf OSCILLATION

A typical oscillogram of broad-band hf oscillations in the discharge is shown in Fig. 3. An analysis of the spectra and of the autocorrelation functions of the oscillations[11] shows that the process constitutes oscillations with periodic components of appreciable amplitude. The correlation time is of the order of the time of flight of the beam through the system, so that in the plasma-beam discharge the electrons interact with an hf field whose essential property is a clearly pronounced regularity.

More details on the character of the oscillations in the plasma-beam system can be obtained by taking into account the fact that the reaction of an electron moving in a traveling-wave field is determined mainly by the amplitude and phase of the field acting on the electron. The condition ω-kv = 0 for the most effective energy exchange

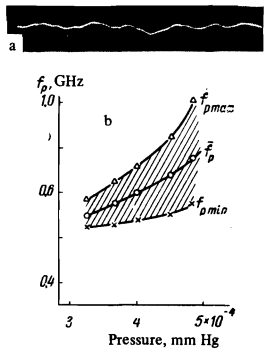

FIG. 2. a) Oscillogram of plasma-density oscillations. Sweep duration 200 μsec; b) range of plasma density oscillations (shaded). f_p—plasma frequency.

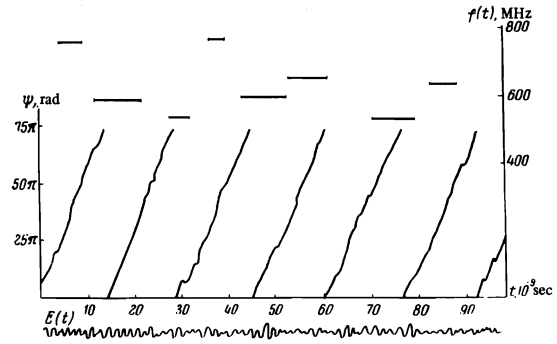

FIG. 3. Typical oscillogram of hf field E(t), the running phase of the oscillations $\psi(t)$, and the instantaneous frequency of the quasiharmonic inclusions f(t).

between the particle and the wave (the synchronism condition) is in itself a condition for the constancy of the phase of the field in the reference frame connected with the particle. It is therefore expedient to represent the field in the plasma in a form such that the field and the amplitude are explicitly given. This circumstance has served as a basis for employment of the phase-frequency analysis method[12] in study of hf oscillations of a plasma-beam discharge.

The gist of the method consists of representing the random process E(t) in the form

$$E(t)=A(t)\cos\psi(t), \tag{1}$$

where the random functions A(t) and $\psi(t)$ are defined by

$$A(t)=[E^2(t)+\hat{E}^2(t)]^{1/2},\quad \operatorname{tg}\psi(t)=\hat{E}(t)/E(t). \tag{2}$$

The quantity $\hat{E}(t)$, which is conjugate to E(t), is constructed by means of a Hilbert transformation[12,13]:

$$\hat{E}(t)=-\frac{1}{\pi}\int_0^\infty\frac{E(t+\tau)-E(t-\tau)}{\tau}d\tau. \tag{3}$$

A(t) and $\psi(t)$ were calculated with a computer.

The results of an analysis of a typical oscillogram of hf oscillations are shown in Fig. 3 in the form of the curve $\psi(t)$ and a plot showing the variation of the running frequency of the process with time, $f(t) = d\psi/2\pi dt$. The $\psi(t)$ curve reveals the presence of quasiharmonic inclusions characterized by linear sections $d\psi/dt$ = const and by abrupt changes of the oscillation phase. From the f(t) plot it is seen that oscillations exist mainly in four frequency regions (530, 580–590, 630–640 and 750–760 MHz), which alternate randomly in time. The lifetime of such quasiharmonic inclusions is $(5-10)\times10^{-9}$ sec, i.e., it spans several periods of the fundamental frequency.

We shall estimate the probability distribution of the excitation of a quasiharmonic inclusion of fixed frequency by summing the lifetimes of the constant-frequency trains.

It turns out here that the maxima of the distribution correspond to the most intense components in the Fourier expansion of the investigated realization (Fig. 4).

The presence of random phase discontinuities between the quasiharmonic inclusions enables us to analyze the nature of the stochastization of the oscillations by making use of the concepts of phase diffusion, which were developed in papers on nonlinear theory of oscillations.[13] The behavior of the phase with time was investigated with a sampling of several hundred oscillograms, constituting an ensemble of realizations of the hf field in one regime. All the oscillograms were artificially phased to the initial instant of time t_0. By virtue of the stochastic character of the oscillations, a dephasing of the ensemble of "generators" takes place in the course of time, and the points representating them diffuse over the phase planes, deviating more and more from the limit cycle representing a monochromatic generator.

Fig. 5 shows histograms of the distribution of the phases of the indicated ensemble at different instants of time, and the theoretical curves

$$w(\psi, \theta) = (4\pi D\theta)^{-1/2} \exp(-\psi^2/4\pi D\theta), \quad (4)$$

which describe the phase diffusion of an autogenerator subject to random uncorrelated fluctuations. Here $\theta = \omega(t-t_0)$ is the dimensionless time and D is the diffusion coefficient. The experimental and theoretical curves are convoluted in the interval $(0, 2\pi)$. The good agreement between the experimental distributions and the curve (4) indicates that the dephasing of the oscillations has a diffusive character, but the rate of diffusion is anomalously large in comparison with the usual radiotechnical generators.

Thus, the results of correlation and phase-frequency analysis of the hf oscillations indicate that a coherent single-mode interaction of the electron beam with the plasma takes place in a plasma-beam discharge. The broadband stochastic form of the oscillatory process is the result of random alternation of quasiharmonic trains, and the transitions between them have the character of uncorrelated phase discontinuities.

3. ELECTRON DISTRIBUTION FUNCTION UNDER CONDITIONS OF A NONSTATIONARY DISCHARGE

The previously established character of the vibrational process leads to the conclusion that other singularities of the single-mode interaction, particularly the oscillatory form of the distribution function, should be realized in a plasma-beam discharge. So far, however, no multiple-hump distribution function has been observed experimentally[1]. When comparing the conclusions of the theory with the experimental results, it must be recognized that the development of beam instability, as noted above, is a nonstationary process under the experimental conditions. One should therefore expect the oscillations on the distribution function likewise to have a non-stationary character under the experimental conditions, since the form of the distribution function is determined by the amplitude and by the frequency spectrum of the waves. We note that the time of measurement of the distribution function in the experiments performed to date has always been larger than the characteristic nonstationarity period, and this has inevitably led to averaging of the measured quantity.

Let us estimate the influence of the inertia of the measurements on the form of the measured distribution function. To clarify the most essential aspects of the phenomenon, it suffices to consider the action of a monochromatic wave of given amplitude on an electron gas with known initial distribution function[2]. Assume that a one-dimensional potential wave $\varphi = \varphi_0 \sin(\omega t - kz)$ propagates in the plasma. The problem consists in determining the space-time evolution of the part of the distribution function in the immediate vicinity of the phase velocity of the wave.

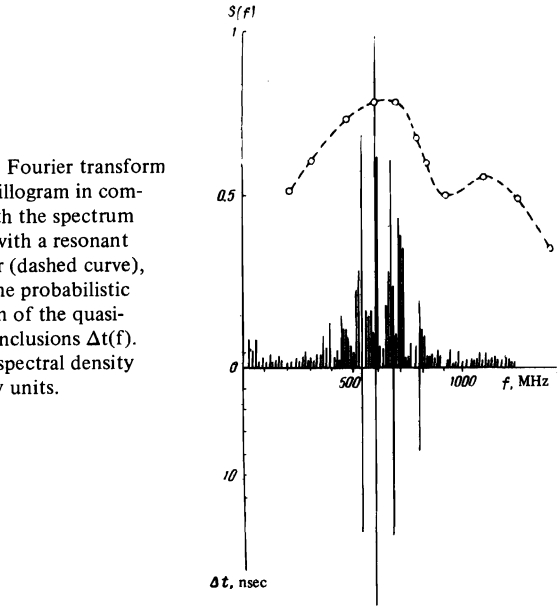

FIG. 4. Fourier transform of E(t) oscillogram in comparison with the spectrum measured with a resonant wave meter (dashed curve), and with the probabilistic distribution of the quasiharmonic inclusions Δt(f). S(f) is the spectral density in arbitrary units.

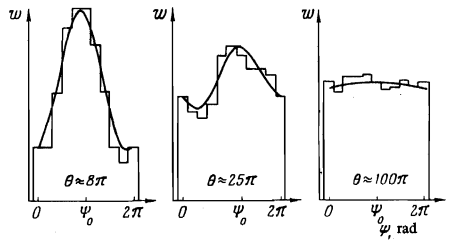

FIG. 5. Time evolution of the phase distribution ψ_0 is the phase of the monochromatic signal at the instant of time θ.

The problem is solved in a co-moving reference frame by numerical integration of the kinetic equation along the phase trajectories. Next, to assess the manner in which the measurement procedure affects the distribution function, we return to the laboratory frame. In terms of the dimensionless variables

$$\tau = (e\varphi_0/m)^{1/2} kt, \quad \xi = kz', \quad \mu = d\xi/d\tau,$$

where z′ is the coordinate in the co-moving reference frame, the first integral of motion is given by[16]

$$\varepsilon_0 = {}^1/_4\mu^2 + \sin^2(\xi/2). \quad (5)$$

The law of motion for the trapped electrons ($\epsilon_0 < 1$) is

$$\tau = F\left[\left(\frac{\mu_0^2}{4} + \sin^2\frac{\xi_0}{2}\right); \ \arcsin\frac{\sin(\xi/2)}{(\mu_0^2/4 + \sin^2(\xi_0/2))^{1/2}}\right] - F\left[\left(\frac{\mu_0^2}{4} + \sin^2\frac{\xi_0}{2}\right); \ \arcsin\frac{\sin(\xi_0/2)}{(\mu_0^2/4 + \sin^2(\xi_0/2))^{1/2}}\right] \quad (6)$$

and for the untrapped electrons ($\epsilon_0 > 1$)

$$\left(\frac{\mu_0^2}{4} + \sin^2\frac{\xi_0}{2}\right)^{1/2} \tau = F\left[\left(\frac{\mu_0^2}{4} + \sin^2\frac{\xi_0}{2}\right)^{-1}; \ \frac{\xi}{2}\right] - F\left[\left(\frac{\mu_0^2}{4} + \sin^2\frac{\xi_0}{2}\right)^{-1}; \ \frac{\xi_0}{2}\right]. \quad (7)$$

Here F is an elliptic integral of the first kind.

Solving (5)–(7) numerically with respect to ξ_0 and μ_0, we use the Liouville theorem, after specifying the initial distribution function, to determine the particle velocity distribution at the chosen instant of time τ and in the chosen cross section (ξ = const) of the phase plane. Figure 6a shows the particle distributions for certain values of τ and ξ. For simplicity, the initial distribution function was approximated by a straight line in the vicinity of the phase velocity of the wave. On the whole, the region of possible values of the distribution function for all τ and ξ is shown dashed in Fig. 6a.

In the experiments, the distribution functions are measured in a fixed (in the laboratory frame) section of the interaction region. We denote the coordinate of the observation point by z_{obs}. The chosen z_{obs} corresponds to

$$\tau_{obs}=\frac{k^2 z_n}{\omega}\left(\frac{e\varphi_0}{m}\right)^{1/2},$$

which now has the meaning of a dimensionless distance from the boundary on which the wave is incident to the observation point. At τ_{obs} = const, as follows from the formula for the conversion to the laboratory frame, the time interval during which the measurements of the distribution function are made is connected with a certain interval $\Delta\xi$:

$$\omega\Delta t_{meas}=-\Delta\xi.$$

This means that all the electrons situated on a phase-plane section of width $\Delta\xi$ have time to pass through the measuring instrument in the interval Δt_{meas}. Since the electron distribution varies with ξ, the form of the experimentally obtained distribution function depends essentially on the value of the interval $\Delta\xi$, i.e., on the inertia of the measurements.

If the measurements are inertialess ($\omega\Delta t_{meas} \ll 1$), the form of the "instantaneous" distribution function depends only on the phase of the wave at which the measurements were performed, i.e., the form of the experimentally measured distribution function will be close to the curves of Fig. 6a with clearly pronounced deep oscillations[9]. In order to get an idea of the form of the distribution function obtained in the case of inertial measurements ($\Delta\omega t_{meas} \gg 1$), it is necessary to carry out averaging, at τ_{obs} = const, over ξ on an interval $\Delta\xi$ of magnitude 2π. Figure 6b shows results of the averaging at $\tau_{obs} = 2\pi$. Notice should be taken here of two circumstances: first, noticeable oscillations remain on the distribution function averaged over the period of the field, and second, at constant parameters of the system (φ_0, ω) the form of the averaged distribution function remains unchanged at all values of Δt_{meas}, and changes only when a transition is made to another section of the interaction region (when τ_{obs} is changed).

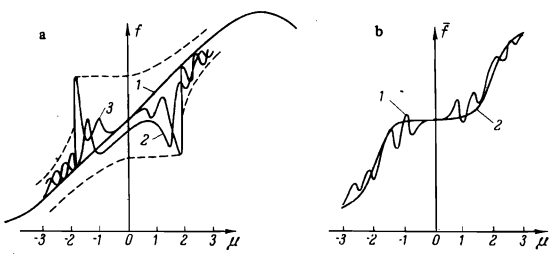

FIG. 6. a) Evolution of instantaneous beam distribution function: 1–initial distribution function $\tau = 0$, 2 – $\tau = 2\pi$, $\xi = \pi/3$; 3 – $\tau = 4\pi$, $\xi = 0$. The dashed lines are the limits of the region of all possible values of the distribution function. b) Form of the averaged distribution function: 1–$T_{lf} \gg \Delta t_{meas} \gg \omega^{-1}$, $\tau_{obs} = 2\pi$; 2–$\Delta t_{meas} \gg T_{lf}$.

The low-frequency plasma-density oscillations that take place in a plasma-beam discharge lead to a time variation of the increment, frequency, and amplitude of the hf waves. Within the framework of the considered model, they can be taken into account by assuming that τ_{obs} is a function of the time while z_{obs} remains constant:

$$\tau_{obs}=\frac{k^2 z_{obs}}{\omega(t)}\left(\frac{e\varphi_0(t)}{m}\right)^{1/2}.$$

This makes it possible to estimate the influence of the inertia of the measurements on the form of the distribution function under conditions when lf oscillations of the system parameters are present. In this case Δt_{meas} turns out to be connected not only with $\Delta\xi$ but also with a certain interval $\Delta\tau_{obs}$, and the form of the experimentally measured distribution function now depends on the ratio of the measurement time to the period of the lf oscillations. To obtain the form of the distribution function at $\Delta t_{meas} \gg T_{lf}$ it is necessary to average both over ξ and over τ_{obs}. Calculation shows that at $\Delta\tau_{obs} \gtrsim 2\pi$ the oscillations on the distribution function become smoothed out, and a horizontal plateau appears in the vicinity of the phase velocity (Fig. 6b). Allowance for the contribution of the untrapped particles leads to a certain slope of the plateau; it must be emphasized, however, that the form of the averaged distribution function remains smooth. In typical experiments, (e.g.,[9,10]), the condition $\Delta t_{meas} \gg T_{lf}$ was satisfied and led indeed to registration of a smooth distribution function.

As is clear from the foregoing, a simple increase of the resolving power in the energy analysis of the electrons in the presence of lf oscillations cannot reveal the theoretically predicted oscillations on the distribution function. We note that "smearing" of the distribution function as a result of the lf density fluctuations should also occur in the case when peaks are produced on the distribution function by interactions with the discrete modes of the plasma-volume oscillations. Therefore the interpretation proposed in[14] for the registered peaks on the distribution functions does not seem convincing enough to us, all the more since the results of an experiment with external beam modulation are in patent disagreement with this interpretation.

Thus, the true form of the distribution function can be experimentally observed, as shown by the considered example, only at $\Delta t_{meas} \ll T_{lf}$

4. RESULTS OF EXPERIMENTAL INVESTIGATION OF THE DISTRIBUTION FUNCTION

The experimental beam-electron-energy distribution function was investigated by the retarding-potential method. The analyzer was structurally incorporated into the collector unit of the installation. The collecting electrode of the analyzer and the external cylinder composed a coaxial line in which the internal conductor was the collecting electrode. The distribution function was measured in two time intervals, about 10^{-4} and 10^{-7} sec.

In the slow-analysis regime, the retarding field was produced by a sinusoidal 50-Hz voltage. A voltage proportional to the retarding voltage was used for the horizontal sweep of an S1-17 oscilloscope. A voltage from a parallel RC network (RC $\sim 10^{-4}$ sec), proportional to the delay current (the current flowing to the Faraday cylinder), was applied to the input of the vertical amplifier. Thus, it was possible to observe and photograph the beam-current delay curve on the oscilloscope screen. The dis-

tribution function was determined by graphic differentiation of the delay curve.

In the case of rapid analysis of the distribution function, the retarding field was produced by a short negative sawtooth pulse. The growth rate of the leading front of the pulse was 6×10^9 V/sec, and the duration of the pulse of 1.5 kV amplitude was on the order of 250 nsec. Thus, the time during which the analysis of the beam-electron velocities was carried out fluctuated between 10^{-8} sec (nonsmeared beam in the absence of a plasma) to 10^{-7} sec in the case of a large spread of the beam velocities as a result of beam interaction with the plasma.

The difference between the conditions under which the slow and rapid analyses of the distribution function were carried out is illustrated in Fig. 7. During the time in which the oscillograms of the delay current were obtained, the plasma density had time to execute many oscillations (the condition $\Delta t_{meas} \gg T_{lf}$ was satisfied), the shape of the delay curve was smooth, and the distribution function obtained by differentiating the delay curve was a smooth-plateaulike curve. In the fast-analysis regime, as seen from a comparison of the oscillograms in Fig. 7, the plasma density does not have time to change significantly. Thus, the relation $T_{lf} \gg \Delta t_{meas} \gg T_{hf}$ is satisfied in the fast analysis of the distribution function.

Oscillograms of the delay current in the fast-analysis regime are shown in Fig. 8 and are arranged from top to bottom in order of increasing system pressures. At sufficiently low pressure (in the absence of plasma) the delay curve takes the form of a step pulse (Fig. 8a) at a retarding voltage U_r = 1 kV, corresponding to the velocity of the unperturbed beam. With increasing pressure, a plasma-beam discharge is ignited and hf and lf oscillations are excited. The intense hf oscillations are also noticeable in the beam current, becoming manifest in a vertial smearing of the beam (Fig. 8d). The shape of the smearing envelope conforms to the hf oscillations registered at the same instant of time by the I2-7 oscilloscope. The decrease of the average slope of the delay curves with increasing pressure indicates that an electron velocity scatter sets in as a result of the interaction with the plasma.

The most significant result of the fast analysis is the nonmonotonic variation of the slope of the delay curve with changing retarding voltage, thus evidencing that the distribution function is multiple-humped. In the reduction of the oscillogram of the decay current for the purpose of obtaining the distribution function, we confined ourselves to representation of the oscillogram in the form of a histogram, since the smearing of the hf beam by the oscillations precludes graphical differentiation with sufficiently small intervals. Figure 9a shows the electron velocity distributions corresponding to the oscillograms of Fig. 8, while Fig. 9b shows the characteristic hf-oscillation oscillograms registered in synchronism with the delay curve.

In the absence of a plasma (Fig. 9a-1) the distribution function has a bell shape corresponding to an energy spread on the order of 40 eV. When the plasma density exceeds the discharge-ignition threshold, the distribution function broadens and hf oscillations are excited, but the amplitude of these oscillations during the initial stage of the instability is too small to be registered with the aid of a high-speed oscilloscope. Figure 9a-2 corresponds to the start of the nonlinear stage of the interaction. The distribution function had a multiple-humped shape with total smearing on the order of 100 eV, while the hf field is nearly monochromatic. With increasing plasma density, the distribution function broadens further, retaining its multiple-humped character. The hf field increases in intensity and acquires the form of an amplitude-modulated oscillation, corresponding to the appearance of satellites in its spectrum. With subsequent expansion of the distribution function, the spectrum of the hf oscillations broad-

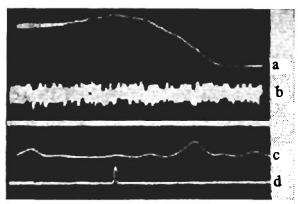

FIG. 7. a) Oscillograms of delay current in the slow analysis of the distribution function; b, c) oscillograms of the plasma-density oscillations; sweep duration 10 msec (b) and 50 μsec (c); d) the pulse duration corresponds to the time of the fast analysis of the distribution function.

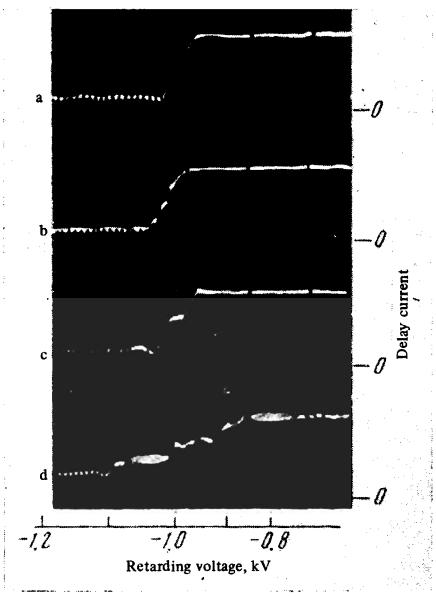

FIG. 8. Oscillograms of delay current. Sweep duration 250 nsec.

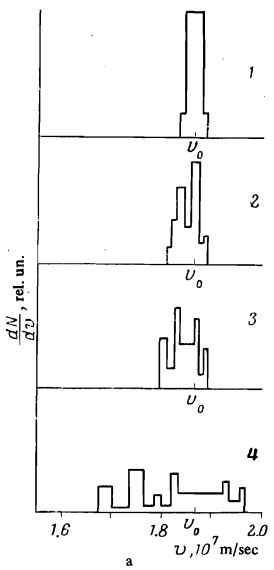

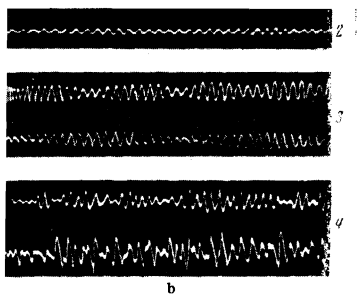

FIG. 9. Electron velocity distribution (a) and corresponding oscillograms of the hf oscillations (b).

ens to such an extent that they acquire the form of a random process.

The broadening of the distribution function proceeds predominantly in the low-velocity direction, but at large values of the plasma density the number of accelerated electrons also increases (Fig. 9a-4). At high plasma density, the oscillations become smoothed out in the vicinity of the initial beam velocity, and they give way to an extended "shelf" (Fig. 9a-4). The remaining peaks are in general broader than of the preceding histograms: the energy scatter of the electrons within a single group reaches 100 eV.

If the pressure and other discharge parameters are fixed, the shape of the delay-current oscillograms (in the fast analysis) does not repeat identically from one triggering of the measuring circuit to another. All that remains the same is the average inclination of the curve to the U_r axis, while the number of sections with different slopes and their mutual placement vary. In the inertial measurement method, the registered curve is an average over an ensemble of high-speed oscillograms: only the general character of the inclination of the curve to the U_r axis is preserved after averaging over the ensemble.

The experiment has confirmed the conclusions drawn from the calculation, namely, the "instantaneous" form of the distribution function does not coincide with its averaged form, but has a more complicated structure that varies with time; the inertial measurement method yields a smooth distribution function.

5. DISCUSSION OF RESULTS

Let us compare the results with the theory. We note first that the very fact that a multiple-humped distribution function has been registered can be explained only on the basis of the nonlinear theory of beam-plasma interaction, in which capture of the electrons by the wave field is taken into account. Both the shapes of the oscillograms of the hf field in the initial nonlinear stage of the instability development (Fig. 9b-2) and the results of the phase-frequency analysis indicate that the interaction in the plasma-beam discharge is in essence coherent and single-mode. Thus, the theory developed in[3-5] can be used to analyze this interaction.

Since the instability develops over the length of the experimental system, and the distribution function is measured at a fixed distance from the plane of injection of the monoenergetic beam into the plasma, the increase of the plasma density is equivalent to an increase of γ or t in the models[3-5] used to consider the development of the instability with time. The growth of the number of peaks on the distribution function with increasing plasma density agrees with the theoretically predicted increase in the number of oscillations with further development of the instability.

The decrease in the absolute values of the peaks and their broadening with increasing plasma density is attributed to a decrease in the density of the "macroparticles"[3] as the beam advances into the plasma.

The formation of a "shelf" in the vicinity of v_0 agrees with the theoretical ideas concerning the mechanism whereby the distribution function becomes smoothed out in time as a result of the increasing role of the Coulomb collisions at large values of $\partial f/\partial v$. Since the first peaks, and consequently the large values of $\partial f/\partial v$, appear in the vicinity of v, it is precisely here that one should expect the first manifestation of their smoothing as a result of diffusion in velocity space due to Coulomb collisions.

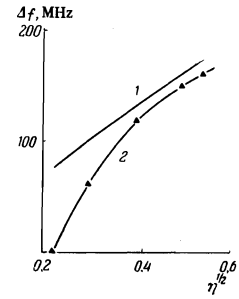

FIG. 10. Spectrum width vs. relative electron energy loss: 1—theoretical curve, 2—experimental curve.

The broadening of the oscillation spectrum, as seen from the form of the oscillograms (Fig. 9b-2, 3) and from the statistical analysis of the time behavior of the oscillation phase, is due to the growth of the amplitude modulation and of the uncorrelated phase discontinuities. Thus, as the instability develops, satellites appear in the wave spectrum and can obviously be connected with the theoretically predicted[6,18] development of instability at the trapped particles. The width of the satellite spectrum can be estimated theoretically from the experimentally measured energy lost by the electrons to excitation of the oscillations. Indeed[6,18],

$$\Delta f \sim (ekE/m)^{1/2}.$$

Assuming that the field of the wave is

$$E = \eta P_0 k (2PR_c)^{1/2},$$

where $\eta = P/P_0$ is the relative beam-power loss and R_c is the coupling resistance of the plasma waveguide, we obtain

$$\Delta f \approx \left(\frac{e}{m}\frac{\omega_p^2}{v_0^2}\sqrt{2\eta P_0 R_c}\right)^{1/2}. \qquad (8)$$

Figure 10 shows a plot of $\Delta f(\eta)$ and the values of the spectral widths determined by computer Fourier transformation of the oscillograms. The discrepancy between the theoretical curve and the experimental data in the initial section is attributed to the fact that expression (8) is an upper-bound estimate, and indicates only the frequency band in which the satellites are located.

Thus, the averaged (macroscopic) characteristics of both the high-frequency oscillations and the beam-electron velocity distribution function mask the true character of the interaction. The investigation of the instantaneous characteristic shows that the beam-plasma interaction is basically a coherent process, in spite of the fact that the averaged characteristics point to a stochastic character of the process. The broadening of the spectrum of the oscillations and their stochastization are the result of development of instability at the trapped particles during the strongly nonlinear stage of the beam instability. Additional randomization and distortion of the characteristics of the hf field and of the beam structure take place in the presence of irregular plasma-density oscillations due to low-frequency types of instability.

[1)]The fine structure of the distribution function of a beam, which is manifested in the presence of peaks, is described in a paper by Levitskiĭ and Nuriev [14]. As will be shown later on, however, this effect has no bearing on the phenomena considered here.

[2)]The self-consistent problem of the transformation of the distribution function in the interaction of a velocity-modulated monoenergetic beam with a plasma is considered in [15].

[3)]Inertialess measurements of the distribution function were performed

by Gabovich and Kovalenko [17] for the case of an interaction of a velocity-modulated beam with a plasma. The results agree with the aforementioned theoretical calculations [15].

[1]A. I. Akhiezer and Ya. B. Faĭnberg, Dokl. Akad. Nauk SSSR **59**, 559 (1949); Zh. Eksp. Teor. Fiz. **21**, 1962 (1951).
[2]W. Drummond, Th. O'neil, J. Malmberg, and J. Thompson, Phys. Fluids **13**, 2422 (1970).
[3]B. B. Kadomtsev and O. P. Pogutse, Phys. Rev. Lett. **25**, 1155 (1970).
[4]Th. O'Neil, Phys. Fluids **8**, 2255 (1965); **14**, 1204 (1971).
[5]L. M. Al'tshul and V. I. Karpman, Zh. Eksp. Teor. Fiz. **49**, 515 (1965) [Sov. Phys.-JETP **22**, 361 (1966)].
[6]V. D. Shapiro and V. I. Shevchenko, ibid. **57**, 2066 (1969) [**30**, 1121 (1970)]; Preprint FTI-72-74, Khar'kov, 1972.
[7]Th. Armstrong, Phys. Fluids **10**, 1269 (1967); **12**, 2094 (1969).
[8]V. D. Shapiro, Zh. Eksp. Teor. Fiz. **44**, 613 (1963) [Sov. Phys.-JETP **17**, 416 (1963)].
[9]S. M. Levitskiĭ and I. P. Shashurin, ibid. **52**, 350 (1967) [**25**, 227 (1967)].
[10]E. G. Shustin, V. P. Popovich, and I. F. Kharchenko, Zh. Tekh. Fiz. **39**, 993 (1969) [Sov. Phys.-Tech. Phys. **14**, 745 (1969)].
[11]V. A. Lavrovskiĭ, V. M. Deev, S. A. Rogashkov, Yu. G. Yaremenko, and I. F. Kharchenko, ibid. **39**, 1586 (1969)].
[12]I. F. Kharchenko, O. V. Betskiĭ, M. M. Tolmachev, and A. T. Polukhin, Radiotekhnika i élektronika **18**, 1507 (1973).
[13]S. M. Rytov, Vvedenie v statisticheskuyu radiofiziku (Introduction to Statistical Radiophysics), Nauka, 1966.
[14]S. M. Levitskiĭ and K. Z. Nuriev, ZhETF. Pis. Red. **12**, 172 (1970) [JETP Lett. **12**, 119 (1970)]; Zh. Eksp. Teor. Fiz. **61**, 190 (1971) [Sov. Phys.-JETP **34**, 99 (1972)].
[15]V. A. Lavrovskiĭ, A. I. Rogashkova, I. F. Kharchenko, and M. B. Tseĭtlin, Radiotekhnika i élektronika **17**, 1776 (1972).
[16]G. Kauderer, Nonlinear Mechanics (Russ. Transl.), IIL, 1961, p. 271.
[17]M. D. Gabovich and V. P. Kovalenko, Dokl. Akad. Nauk. SSSR **199**, 799 (1971) [Sov. Phys.-Dokl. **16**, 640 (1972)]
[18]N. I. Bud'ko, V. I. Karpman, and D. R. Shklyar, Zh. Eksp. Teor. Fiz. **61**, 1463 (1971) [Sov. Phys.-JETP **34**, 778 (1972)].

Translated by J. G. Adashko
232